Research Article

Chaohui Wang*, Qian Chen*, Tengteng Guo, and Lian Zhang

Preparation and adsorption properties of nano-graphene oxide/tourmaline composites

https://doi.org/10.1515/ntrev-2021-0113
received September 15, 2021; accepted October 10, 2021

Abstract: This research addresses the asphalt smoke emission in the process of asphalt pavement construction. The nano-graphene oxide (GO)/tourmaline composites were prepared to alleviate the asphalt smoke emission and improve the construction environment. The macrocharacteristics and micromorphology of the composites were analyzed, and their optimal preparation process was determined. Using material microanalysis methods, such as X-ray diffractometer, Raman spectroscopy, and Fourier transform infrared spectrometer, the structural characteristics and material composition of the composites were studied. The adsorption properties of the composites on asphalt smoke were clarified. It will provide technical support for the improvement of infrastructure construction environment. The results show that 3-aminopropyl triethoxysilane is superior than hexadecyl trimethyl ammonium bromide in surface modification of tourmaline. During the composite process, surface modifiers and GO had no significant effect on the structure of tourmaline. GO could enhance the adsorption properties of tourmaline on asphalt smoke. When the GO content was 1.5 wt%, the improvement was the largest, which is 17.42%. At that time, the emission-reduction rate of asphalt smoke reached 41.11%.

Keywords: nanocomposites, graphene oxide, tourmaline, adsorption properties

1 Introduction

Transportation infrastructure plays a vital role in human life and world economic development [1]. Asphalt pavement is the main component of transportation infrastructure. During the construction process of asphalt pavement, asphalt is heated to high temperature, which will release a large amount of asphalt smoke [2]. This endangers the health of staff and causes pollution to the surrounding environment [3,4]. In recent years, the researches on emission reduction in the construction of asphalt pavement have gradually received more attention [5–9]. In response to this, scholars have proposed the modifiers suitable for traditional hot-mix asphalt mixtures that can effectively adsorb asphalt smoke [10]. It provides an effective way to solve the above-stated technical problems, but it needs to be further studied.

Among many modifiers with adsorption properties, tourmaline inorganic particle is unique and has been widely studied and applied in the field of environmental protection [11,12]. Scholars have applied it to the field of road materials and studied the pavement performances and environmental effects of its modified asphalt and mixtures [13,14]. Ding *et al*. analyzed the microstructure, chemical composition, and thermal properties of the tourmaline-modified asphalt [15]. Ye *et al.* studied the rheological characteristics and aging resistance of tourmaline-modified asphalt [16]. Zhao *et al.* and Zhu investigated the modification mechanism of tourmaline powder on base asphalt [17,18]. Wang *et al.* and Chen *et al.* prepared tourmaline-modified asphalt mixture with environmental effects and systematically evaluated its emission-reduction efficiency [19–22]. The other study was conducted to investigate the functional, piezoelectric, and thermoelectric properties of a tourmaline-modified asphalt binder and the corresponding asphalt mixtures [23]. The above researches shows that when tourmaline is used in modified asphalt mixture, it can give its emission-reduction effect without losing pavement performance. Moreover, the higher the content of tourmaline, the better its adsorption properties to asphalt smoke. When the content of

* **Corresponding author: Chaohui Wang,** Department of Road Engineering, School of Highway, Chang'an University, Xi'an 710064, China, e-mail: wchh0205@chd.edu.cn
* **Corresponding author: Qian Chen,** Department of Road Engineering, School of Highway, Chang'an University, Xi'an 710064, China, e-mail: 2016121160@chd.edu.cn
Tengteng Guo, Lian Zhang: Department of Road Engineering, School of Highway, Chang'an University, Xi'an 710064, China

Open Access. © 2021 Chaohui Wang *et al*., published by De Gruyter. This work is licensed under the Creative Commons Attribution 4.0 International License.

tourmaline is 20–25 wt% of asphalt, the emission-reduction rate of asphalt smoke can reach 40–50%. However, the high content (>20 wt%) of tourmaline will cause the deterioration of the service performance of asphalt pavement. Therefore, how to further improve the adsorption properties of tourmaline at low content (about 15 wt%) is a research topic worth exploring.

Li *et al*. discussed the efficient adsorption behavior of tourmaline and the ion exchange in the process [24]. Li *et al*. prepared tourmaline/g-C_3N_4/$BiVO_4$ composites to enhance the adsorption effect of tourmaline on pollutants [25]. Chen *et al*. studied the adsorption and its mechanism of Pb(II) by tourmaline-montmorillonite composite [26]. Li *et al*. studied the charge transfer law in tourmaline composites [27]. Wang *et al*. analyzed the correlation between the amount of negative ions released by tourmaline and the band gap, carrier concentration, and mobility, respectively [28]. The current research shows that the adsorption properties of tourmaline mainly rely on the released negative ions to adsorb pollutants [29]. Its electrical properties are the key indicators and need to be further improved.

One of the key technical approaches to improve the negative ion release and adsorption properties of tourmaline is to enhance its electrical properties. Graphene (G) and graphene oxide (GO) have significant conductivity [30]. They have been widely used in composites, nanoelectronic devices, catalyst carriers, sensors, and energy storage devices [31–33]. The modification of G or GO can effectively improve the electrical properties and surface activity of inorganic particles [34]. The prepared high-performance composites have excellent application prospects. If the excellent electrochemical properties of G or GO can be used, the adsorption properties of tourmaline will be further improved. Considering the economic cost of the material, GO is preferred as the modified material in this research.

At present, there are few reports on the preparation methods of GO/tourmaline composites, but tourmaline belongs to inorganic particles. The preparation methods of inorganic particle/GO composites can be referenced. Their main preparation methods were electrostatic self-assembly, hydrothermal synthesis, high-energy ball milling, sol–gel, melting metallurgy, and chemical deposition [35–39]. These studies indicated that the processes of hydrothermal synthesis and electrostatic self-assembly are similar, but the former needs high-pressure reactor and other containers. In sol–gel process, the precursor is used to form oxides and then assembled together. Hydrothermal synthesis, sol–gel, melting metallurgy, and chemical deposition have a narrow application range, high cost, and high process requirements. They are not suitable for large-scale promotion and application. Based on this, the electrostatic self-assembly and high-energy ball milling are mainly concerned.

According to the above-stated motivation, the primary objective of this research is to further enhance the adsorption properties of tourmaline on asphalt smoke, thereby significantly improving the construction environment of asphalt pavement. The surface modifier of tourmaline with obvious effect was selected by the zeta potential. The preparation method of composites was proposed, and GO/tourmaline composites were prepared. The macrocharacteristics and micromorphology of composites were analyzed, and the optimal preparation process was determined. Based on material microanalysis methods, the structural characteristics and material composition of composites were studied. The adsorption properties of asphalt smoke of composites were clarified. It laid a solid foundation for further promotion and application of tourmaline in the field of environmental friendly materials.

2 Experiment materials and methods

The surface of tourmaline was modified by modifiers, which changed the charge property of tourmaline in aqueous solution. The positively charged modified tourmaline and negatively charged GO were combined by an electrostatic attraction among particles. The exfoliated GO adhered to large-sized tourmaline particles. In addition, nano-sized tourmaline can be intercalated between GO layers. Finally, GO/tourmaline composites were prepared.

2.1 Main raw materials

Tourmaline is a kind of borosilicate mineral with a ring structure, and its chemical formula was $Na(Mg,Fe,Mn,Li,Al)_3Al_6[Si_6O_{18}][BO_3]_3(OH,F)_4$. It was supplied by Hebei Lingshou Tourmaline Co., Ltd (Industrial Zone, Shijiazhuang City, Hebei Province, China), and its parameters are shown in Table 1.

GO was prepared from natural graphite by optimized Hummers method. It was supplied by Suzhou Tanfeng Graphene Technology Co., Ltd (Suzhou City, Jiangsu Province, China), and its parameters are shown in Table 2. According to efficacy improvement and material cost, the content of GO was determined as 0.5–1.5 wt% of tourmaline [40].

In this research, the electrostatic self-assembly method was used. G materials and tourmaline have the same negative potential. Therefore, some modifiers are needed to change the

Table 1: Parameters of tourmaline

Material	Color	Mohs hardness	Negative ion release	Emissivity (ε)	Fineness
Tourmaline	Black powder	7.0–7.2	800–1,000 cm^{-3}	84–94	2,000 mesh

Table 2: Parameters of GO

Material	Purity	Thickness	Lamella diameter	Number of plies	Specific surface area	Morphology	Color
GO	>95 wt%	3.4–7 nm	10–50 μm	6–10	100–300 $m^2 g^{-1}$	Powder	Dark brown

potential of the material surface. The surface of tourmaline was modified by two kinds of commonly used modifiers: (1) 3-aminopropyl triethoxysilane modifier (KH-550) was colorless and transparent liquid and was sensitive to humidity and corrosive. (2) Hexadecyl trimethyl ammonium bromide modifier (cetyltrimethylammonium bromide [CTAB]) was a white powder, which is soluble in water and produced a large amount of foam during concussion. It had obvious compatibility with cationic, nonionic, and amphoteric surfactant modifiers. They were supplied by Shaanxi Xinhui Chemical Glass Instrument Co., Ltd (Xi'an City, Shaanxi Province, China), and their parameters are shown in Table 3.

Anhydrous ethanol was a colorless and clear liquid. It was easily soluble in water and can be miscible in water and various organic solvents in any proportion. It was used as a solvent in the powder material-modification process or as an auxiliary agent in the ball milling process. It was supplied by Shaanxi Xinhui Chemical Glass Instrument Co., Ltd, and its parameters are shown in Table 4.

2.2 Preparation method

The surface modifier with a better effect was selected. Based on this, GO/tourmaline composites were prepared. The preparation process of $GO_{1.0}/T_{100}$ (GO:T = 1:100, weight ratio) was taken as an example. The preparation process was as follows.

2.2.1 Assembly of suction filtration device

Buchner funnel, air compressor, filtering flask, wide-mouth bottle, and filter paper were used to assemble the suction filtration device. It was used for the filtration and purification of modified powder.

2.2.2 Surface modification of tourmaline

(1) About 100 g tourmaline was added to 800 mL absolute ethanol to obtain a suspension. It was stirred at a high speed (500 rpm) in a thermostatically heated magnetic stirrer for 20 min to obtain a uniformly mixed tourmaline suspension; (2) about 100 mL absolute ethanol and 100 mL water were mixed in a ratio of 1:1. About 20 g surface modifier was added into the mixed solution of absolute ethanol and water. After the mixture was well stirred, it was added to the tourmaline suspension in batches; (3) the above mixed suspension was stirred at 50°C for 6 h. After the reaction, the mixed solution was filtered. Absolute

Table 3: Parameters of surface modifier

Material	Alternative name	CAS NO	Molecular formula	Molecular weight
3-Aminopropyl triethoxysilane	KH-550	919-30-2	$C_9H_{23}NO_3Si$	221.37
Hexadecyl trimethyl ammonium bromide	CTAB	57-09-0	$CH_3(CH_2)_{15}N(Br)(CH_3)_3$	364.45

Table 4: Parameters of anhydrous alcohol

Material	Melting point	Relative density	Boiling point	Relative vapor density	Molecular weight	Ignition temperature
Anhydrous alcohol	−114.1°C	0.79 g cm^{-3}	78.3°C	1.59 g cm^{-3}	46.07	363°C

ethanol and deionized water were used to repeatedly wash the filtrated products; and (4) the obtained filter cake was dried at 80°C and milled by a planetary ball mill at low speed (200 rpm) for 10 min. The modified tourmaline was obtained through a 200-mesh sieve.

2.2.3 Dispersion of GO

The dispersive aqueous solution of GO with a concentration of 1 mg mL^{-1} was prepared. The prepared GO aqueous solution was ultrasonically vibrated at room temperature for 3 h in an ultrasonic dispersant to obtain a uniformly dispersed GO suspension, which was put into a reagent bottle for use.

2.2.4 Preparation of GO/tourmaline composites

(1) The modified tourmaline was added to deionized water and stirred at high speed to prepare a uniform suspension of modified tourmaline. The content of modified tourmaline was adjusted to 10 wt%. It was weighed 200 g for standby; (2) about 200 mL GO suspension was slowly added to the modified tourmaline suspension under high-speed vibration and stirring; (3) after adding, the stirring speed was maintained, and the reaction was set for 2 h. The filtered products were collected and repeatedly washed with deionized water; and (4) the obtained filter cake was dried at 80°C and milled by planetary ball mill at low speed (200 rpm) for 10 min to make composite powder redispersible evenly. GO/tourmaline composite was obtained through a 200-mesh sieve.

2.3 Experiment equipment and methods

2.3.1 Zeta potential tester

The total number of particles at different potentials was measured by zeta potential tester (Figure 1). After data processing, zeta potential distribution diagrams of materials in solvent were obtained. The instrument was Zetasizer Nano S90 produced by Malvern company, UK. The measurement range of zeta potential was 0–150 mV. The measurement range of particle size was 3 nm to 10 μm. The test temperature was 25°C.

2.3.2 Field-emission scanning electron microscopy

It was mainly used to observe the fine morphology, fracture, and internal structure of materials. The instrument was Verios 460 scanning electron microscope (SEM) produced by FEI (Field Electron and Ion Co.) company, USA. The resolution of secondary electronic image was 1.0–1.4 nm, and the magnification was 20–800,000. In addition, the X-ray

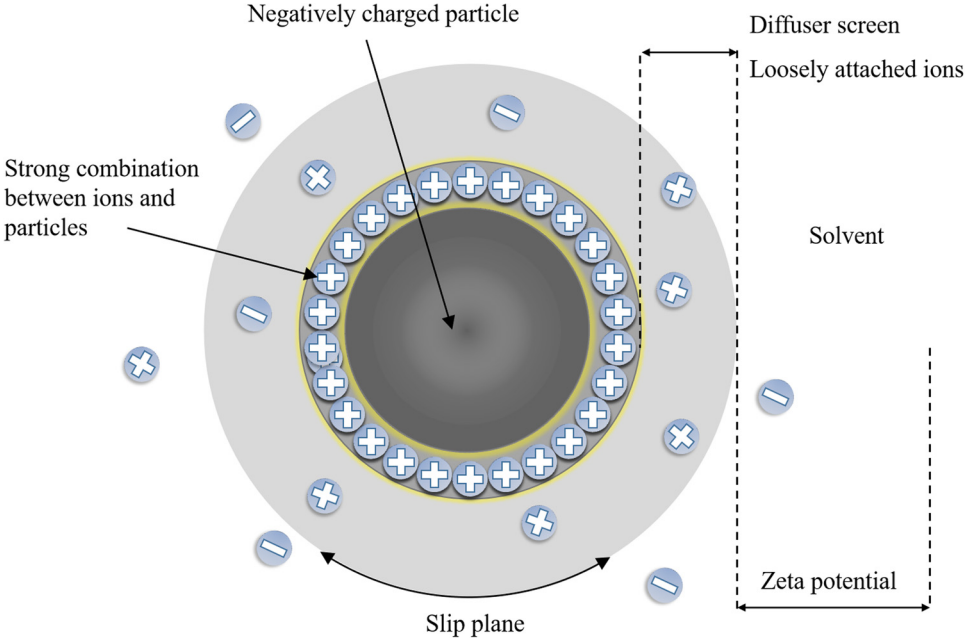

Figure 1: Schematic of zeta potential.

energy-dispersive spectrometer equipped with the instrument was used for qualitative and semiquantitative analysis of sample composition and the analysis element range was Be4-U92.

2.3.3 X-ray diffractometer (XRD)

It was mainly used for qualitative and quantitative analyses of various materials. The internal structure and morphology of materials were obtained by analyzing the diffraction patterns. To improve the accuracy of results, it was necessary to grind the powder before the test. The instrument was D8 XRD produced by Bruker AXS in Germany. The equipment used Cu target ray source. The scanning range was 10–80°. The angle accuracy was 0.0001°. The scanning speed was 4° min^{-1}. The step size was 0.02°.

2.3.4 Laser microscopic confocal Raman spectrometry

It was mainly used for the determination and confirmation of material composition. The test material was placed under the Raman spectrometer, and the spectrum was tested from different points of the sample. The instrument type was Renishaw-inVia. The laser wavelength was 532 nm, the measurement range was 100–4,000 cm^{-1}, and the accuracy was 2 cm^{-1}.

2.3.5 Fourier transform infrared (FT-IR) spectrometry

FT-IR was used to determine the molecular structure of substances. The experiment materials should be dried. After drying 0.2 mg experiment materials and 150 mg KBr at 105°C for 3 h, they were ground and mixed evenly with a mortar. A small amount of mixed powder was put into the die, and the sample was prepared by holding the pressure of 10 t cm^{-2} for 2 min. The instrument was ALPHA II FT-IR produced by Bruker Optics in Germany. SNR was 50,000:1. The resolution was 0.8 cm^{-1}. The wavenumber range was 7,500–375 cm^{-1}.

2.3.6 Adsorption test of asphalt smoke

According to GB 31570–2015 [41], asphalt smoke concentration was characterized. The adsorption properties of tourmaline and its composites on asphalt smoke were evaluated by analyzing the change of asphalt smoke concentration. The recommended content of tourmaline materials was 15 wt% [21]. As the absorption solution, 20 mL benzene solution was added into the absorption bottle. Then, asphalt (SK-70#) was heated to 160°C to produce asphalt smoke. The air sampler was used to extract asphalt smoke into the absorption bottle. The collection speed was 0.5 L min^{-1}, and the collection time was 0.5–2 h. Next, the benzene-asphalt smoke solution in the absorption bottle was poured into the evaporating dish. It was dried (80°C) and weighed. The concentration of asphalt smoke was calculated by equation (1).

$$\alpha = \frac{(m_0 - m_1) \times 10^3}{0.5t \times 10^{-3}}, \quad (1)$$

where α was concentration of asphalt smoke, mg m^{-3}; m_1 was weight of evaporating dish after drying, g; m_0 was weight of evaporating dish, g; and t was collection time of asphalt smoke, min.

3 Results and discussion

3.1 Selection of surface modifier

The key of electrostatic self-assembly was the surface modification of inorganic particles. Inorganic particles and GO should have opposite electrical properties in solution. Zeta potentials of G and GO were measured. The changes of zeta potential before and after tourmaline modification were compared. The test results were shown in Figures 2 and 3 and Table 5. The suitable surface-modification scheme of tourmaline was determined. For standard writing, KH-550-modified tourmaline was abbreviated as KT, and CTAB-modified tourmaline was abbreviated as CT.

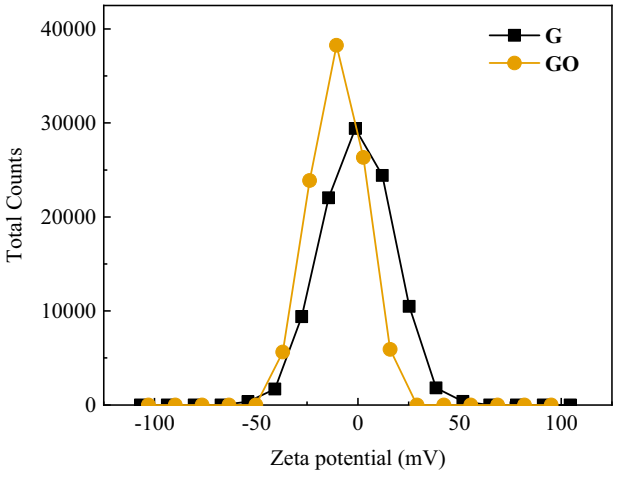

Figure 2: Zeta potential distribution of G and GO.

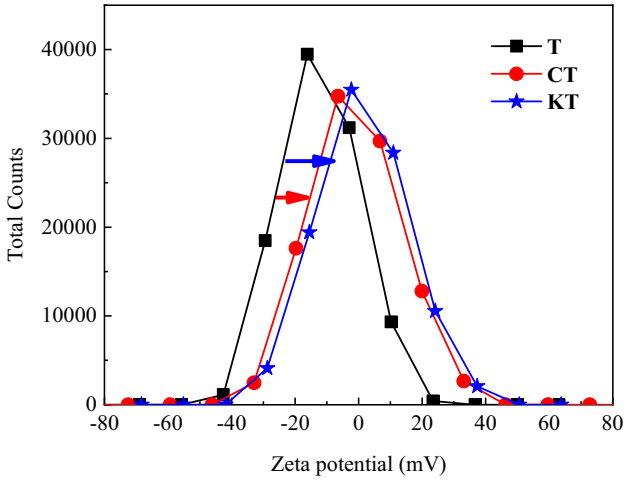

Figure 3: Zeta potential distribution of tourmaline before and after modification.

Table 5: Zeta potential test results

Test object	G	GO	T	CT	KT
Zeta potential (mV)	−0.54	−10.2	−12.22	−1.13	+1.41

According to Figure 2 and Table 5, G was approximately electrically neutral in the solvent, and the absolute value of zeta potential was relatively small. Compared with G, the potential distribution of GO shifted to the left, and the zeta potential was −10.2 mV. It indicated that G is not suitable for the preparation of composites by electrostatic self-assembly. The final zeta electrical change of KT showed that KH-550-modified tourmaline and GO meet the basic conditions for electrostatic self-assembly of composite materials. From Figure 3, the potential of tourmaline in solvent was obviously lower than 0, whereas the zeta potential after surface modification shifted to the right. KT was superior than CT in changing the whole electrical property. According to zeta potential in Table 5, KH-550 changed the surface potential of tourmaline from −12.22 to +1.41 mV. This confirmed the judgment that KH-550 has a better modification effect. It could be inferred that there is a strong electrostatic adsorption between GO and KT after mixing. The electrostatic effect made KT adsorb GO. In addition, the two were combined by the reaction of chemical groups. This allowed a single layer or a few layers of GO to be coated on KT surface, thereby obtaining GO/KT composites. Therefore, silane coupling agent (KH-550) was selected as the final surface modifier of tourmaline.

In the preparation of GO/KT composite, KH-550 was hydrolyzed in water, and the generated silanol reacted with the hydroxyl groups on the surface of tourmaline to form ether bond. This formed a strong chemical connection and changed the electrical properties of tourmaline surface. There were a large number of oxygen-containing functional groups on the surface of GO, such as carboxyl groups and phenolic hydroxyl groups. In the aqueous solution, these groups were prone to ionization, which made the surface of GO negative [42]. This made the modified tourmaline, and GO can be synthesized by electrostatic self-assembly. In addition, the methoxyl group at one end of KH-550 can be hydrolyzed to form silicon hydroxyl group, which condensed with the hydroxyl group on the tourmaline surface. The amino groups at the other end of KH-550 can react with epoxy functional groups on the GO surface [43]. KH-550 acted as a bridge to connect GO to the surface of tourmaline by a chemical bond.

3.2 Morphology characteristics of composites

3.2.1 Macrophenomenon

Figure 4 showed the powder photos of tourmaline, KH-550-modified tourmaline, and GO/tourmaline composites. The surface morphology of tourmaline was not changed by KH-550. The overall appearance was still gray and white. This was because the tourmaline samples come from raw

Figure 4: Macromorphology of tourmaline before and after modification.

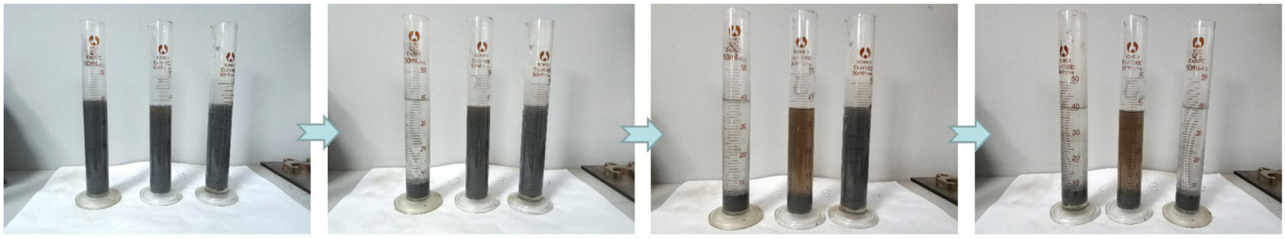

Figure 5: Suspension standing phenomenon (from left to right: GO/KT composites, GO/T composites, and KT).

ore, and there are gray white powder impurities in tourmaline powder. The surface color of tourmaline modified by GO was deepened and uniform. With the increase of GO content, the color of composites deepened gradually. The GO/T (or GO/KT) composites presented in the following were composed of G (or GO) and tourmaline with a weight ratio of 1:100.

The GO/T powder prepared by mechanical mixing method was used as the control group, and the composite effect of GO/KT powder prepared by electrostatic self-assembly method was explored. KT, GO/T, and GO/KT were used to prepare three kinds of aqueous solutions (1 g mL^{-1}), which were stirred and dispersed evenly and then placed in a measuring cylinder. The dispersion of the mixed solution was observed after standing for different times, as shown in Figure 5.

From Figure 5, after standing for 5 min, GO/KT suspension began to stratify. The upper layer was clear liquid, and the lower layer was modified tourmaline powder. In contrast, KT and GO/T suspensions were still turbid. After standing for 15 min, GO/T suspension also showed obvious stratification phenomenon, but it was different from GO/KT suspension. The upper solution of GO/T was brown yellow, not clear. This showed that simple mechanical mixing cannot effectively load G onto the surface of tourmaline. The two separated in the ethanol solution due to their own weight. The upper brown yellow solution was GO aqueous solution. At the same time, it also indirectly proved the success of electrostatic self-assembly of GO and KT. After standing for 30 min, KT suspension showed obvious stratification. The increase of delamination time indicated that KH-550 can effectively modify the surface properties of tourmaline and improve its dispersion in aqueous solution.

3.2.2 Micromorphology

To further verify the modification effect of GO on tourmaline, the surface morphology of samples was amplified and observed.

In Figure 6(a), GO was in the form of flakes with a flake diameter between 5 and 15 μm. They were multiparticle accumulation, and their thickness was relatively thick, showing the phenomenon of multilayer accumulation. They had not been peeled off sufficiently. This kind of GO was difficult to participate in the reaction due to its own size and thickness, and it cannot demonstrate the superiority of G two-dimensional materials. In Figure 6(b), after 3 h of ultrasonic dispersion, the wrinkles on GO surface can clearly be observed. Compared with GO that is not ultrasonically dispersed, its flake diameter had not

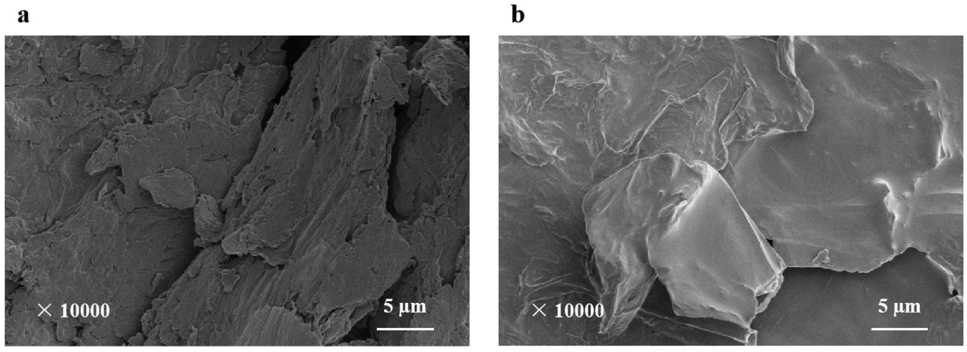

Figure 6: SEM images of GO: (a) before ultrasonic dispersion and (b) after ultrasonic dispersion for 3 h.

changed significantly, but its thickness was reduced. Its peeling layer number was higher than that of untreated GO, and its specific surface area improvement effect was obvious. It showed that the peel off effect of GO was significant after ultrasonic dispersion, forming a similar single-layer GO, which can effectively improve its performance.

From Figure 7(a), tourmaline presented irregular distribution, with flake, blocky, and prismatic morphology. There were irregular edges and corners on the surface, and the size was mostly between 2 and 10 μm. Additionally, due to its own polarization, tourmaline surface adsorbed irregular particles, which may be fine particles in the process of tourmaline grinding. From Figure 7(b), the surface of tourmaline treated by KH-550 had no significant change. It indicated that KH-550 does not change the surface morphology of tourmaline, only changes its surface chemical characteristics.

In Figure 7(a)–(c), it was found that the preparation process of GO/KT composites does not damage the original surface morphology of tourmaline. In Figure 7(c), it was obvious that layered materials are attached to the surface of tourmaline. The surface morphology was further magnified (×50,000), and the characteristics of surface wrinkles were observed, as shown in Figure 7(d). According to Figures 6 and 7, it was determined that the above-layered materials are GO with lamellar structure. This indicated that GO is effectively attached to tourmaline surface after electrostatic assembly, and the lamellar layers are effectively peeled off. At the same time, there were few separate GO lamellar structure, which verified the interaction between GO and modified tourmaline.

3.3 Material composition of composites

3.3.1 XRD analysis

The X-ray diffraction patterns of different materials before and after the test were tested to study the composition characteristics of GO/KT composites prepared by electrostatic self-assembly method.

Figure 8 showed the XRD pattern of GO. There was a strong diffraction peak at 2θ of 11.306°, which was the characteristic peak formed by restacking GO after drying. Moreover, there was a small peak at 2θ of 42.551°, which was the amorphous peak of graphitized carbon. The peak intensity was weak. According to Bragg equation ($2d \sin\theta = \lambda$, X-ray wavelength = 1.5406), the interlayer spacing of GO was 0.78 nm, which was much higher than that of ordinary graphite (2θ is about 26.5°) [28]. It indicated that a large number of oxygen-containing groups are intercalated between GO flakes. Under the condition of ultrasonic dispersion, the lamellar was easier to peel

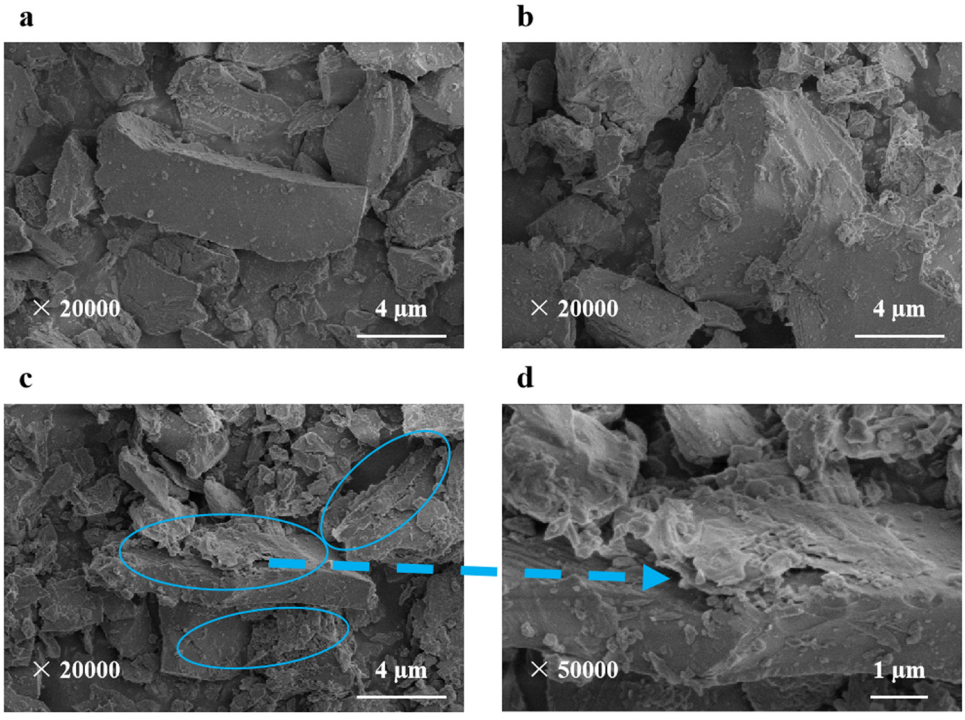

Figure 7: SEM images: (a) tourmaline, (b) KH-550-modified tourmaline, and (c and d) GO/KT composites.

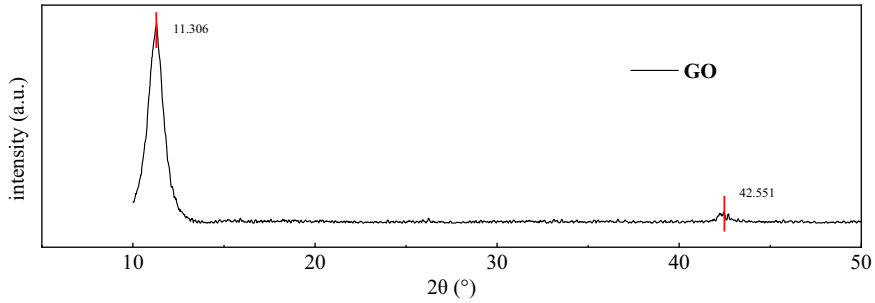

Figure 8: XRD pattern of GO.

off. This provided a prerequisite for the exfoliation of single-layer GO.

Figure 9 showed the X-ray diffraction pattern of tourmaline and the phase retrieval results obtained by Jade software (Materials Data, Inc., Livermore, California, United State). According to search results, the substances with high matching value were selected. The retrieval results of standard cards were compared with the test

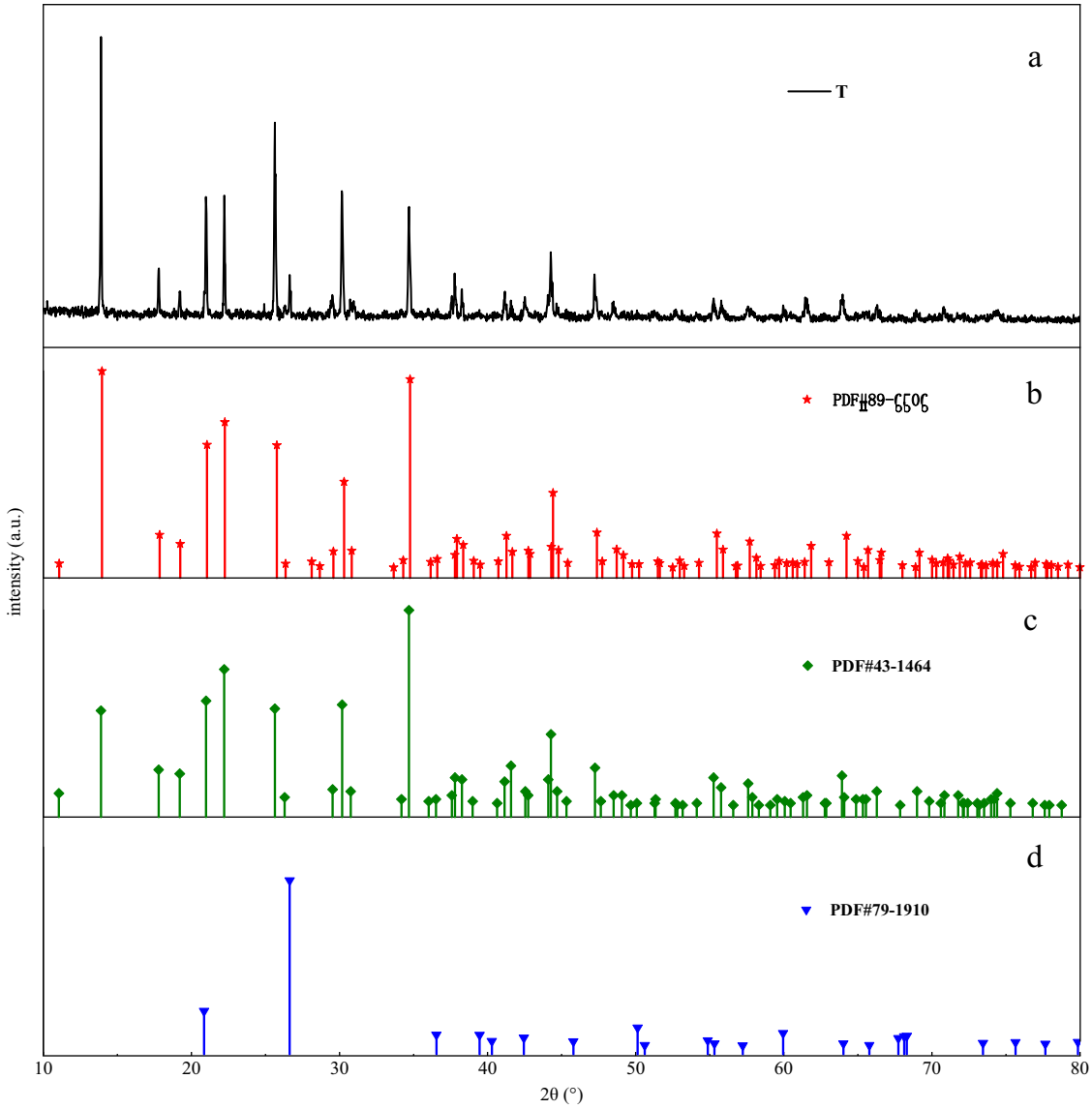

Figure 9: XRD patterns of tourmaline and its corresponding power diffraction file (PDF) card.

Table 6: Chemical composition of tourmaline powder

Chemical composition	SiO_2	Al_2O_3	Fe_2O_3	Na_2O	F	MgO	CaO	MnO
Proportion	40.5004	34.1202	20.4223	2.1322	1.0184	0.5900	0.3890	0.2638
Chemical composition	K_2O	TiO_2	ZnO	SnO_2	P_2O_5	Ga_2O_3	Y_2O_3	SrO
Proportion	0.2612	0.1500	0.0633	0.0379	0.0226	0.0153	0.0085	0.0050

results. In Figure 9(a)–(c), it can be seen that the diffraction peaks and their intensities of standard cards match those of tourmaline samples. Among them, the matching results of the three strongest peaks in Figure 9(b) with the tourmaline sample were the best, and their standard diffraction peaks almost coincide with those of the sample. Based on the chemical composition table obtained by X-ray fluorescence spectrometry, the main crystal image of the sample was $Na_{0.42}Fe_3Al_6B_3O_9Si_6O_{18}(OH)_{3.65}$. The retrieval number of standard PDF card was #89-6506. In addition, when the 2θ was 26.636°, the sample had a diffraction peak (101). According to Figure 9(d) and search results of X-ray photoelectron spectroscopy, it can be judged that there may be a small amount of SiO_2 phase in the sample. The chemical composition of tourmaline powder was shown in Table 6.

Figure 10 showed the changes of XRD pattern of tourmaline before and after modification. The XRD patterns of tourmaline modified by KH-550 and GO did not change significantly. There was no obvious displacement or intensity change of the corresponding characteristic peak. The results showed that the structure of tourmaline is not destroyed during the process of electrostatic self-assembly. The characteristic peaks in XRD patterns were summarized in Table 7. The addition of GO had no significant effect on characteristic peak strength of tourmaline. In addition, from the abscissa of each peak, the addition of GO made the characteristic peak of tourmaline have a small angle deviation. This phenomenon may be due to the intercalation of tourmaline crystals with smaller sizes between GO flakes [44].

3.3.2 Raman spectroscopy analysis

The measured Raman spectra were shown in Figure 11. The characteristic peaks of GO were summarized in Table 8, and the characteristic values of I_D/I_G were calculated.

In Figure 11, GO clearly showed two characteristic peaks at 1346.91 and 1587.29 cm^{-1}. D peak can reflect the degree of structural defects and disorder of carbon plane, whereas G peak can reflect the order degree of carbon plane. After GO was compounded with tourmaline, the characteristic peak intensity decreased at the positions of D peak and G peak of the original GO, but the width did not change significantly. This indicated that GO adheres to the surface of tourmaline and has a corresponding change [45]. In addition, the relative strength of D peak decreased with the increase of the GO content. The results showed that the increase of the GO content in the composites is helpful to improve its physical properties.

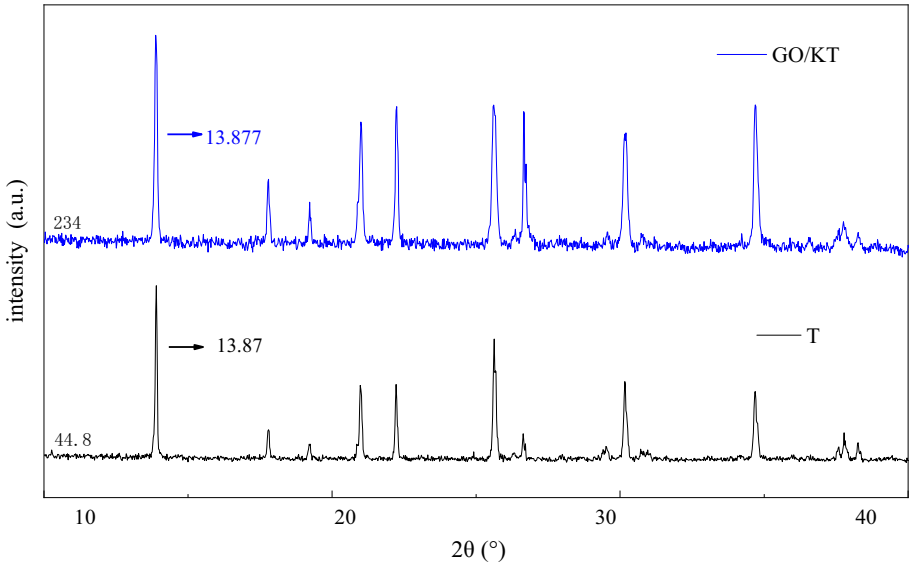

Figure 10: XRD pattern of GO/KT composites and T.

Table 7: Change of peak line position before and after modification of tourmaline

Materials	Peak 1	Peak 2	Peak 3	Peak 4	Peak 5	Peak 6	Peak 7
T	13.87°	34.675°	25.589°	22.228°	20.975°	30.146°	26.65°
GO/KT	13.877°	34.685°	25.607°	22.238°	20.998°	30.194°	26.652°

According to Figure 11 and Table 8, G peak did not change significantly, but D peak had a certain red shift with the increase of the GO content. The I_D/I_G of $GO_{0.5}$/KT, $GO_{1.0}$/KT, and $GO_{1.5}$/KT showed a decreasing trend, which indicated that the disorder degree of materials decreased. The I_D/I_G in carbon materials is directly proportional to the structural defects and inversely proportional to their size. According to the change of I_D/I_G, the average size of GO decreased after it was compounded with tourmaline. This indicated that a large number of small size or exfoliated GO were produced in preparation process. With the increase of the GO content, these small-sized GO will not peel off from the surface of tourmaline due to drying and dispersion problems, and the defects will reduce. In addition, there were more oxygen-containing groups on the surface and edge of GO, which made it easier to form a three-dimensional structure with tourmaline, thus reducing the disorder structure.

3.3.3 FT-IR analysis

When tourmaline samples were irradiated with infrared light, the chemical bonds or functional groups in the molecules appeared stretching the vibration mode. Different chemical bonds or functional groups had various absorption frequencies and were in different positions in infrared pattern. The information about the changes of chemical bonds and functional groups can be obtained. At the same time, according to the status of characteristic peaks, the quality of modification effect was judged, and the existence forms of silane and GO on tourmaline surface were known. The changes of surface functional groups of powder before and after modification were compared. The surface modification effect of tourmaline was verified, and its mechanism was analyzed.

Figure 12 showed that tourmaline has significant infrared activity at wave numbers of 500, 750, 1,000, 1,400, and 3,560 cm^{-1}. Among them, the characteristic absorption band of Si–O bending vibration was mainly near the wave number of 500 cm^{-1}. The characteristic absorption band of Si–O–Si skeleton vibration was mainly near the wave number of 750 cm^{-1}. The characteristic absorption band of O–Si–O stretching vibration was mainly near the wave number of 1,000 cm^{-1}. The characteristic absorption band of BO_3 stretching vibration was mainly near the wave number of 1,400 cm^{-1}. The characteristic absorption band of O–H stretching vibration was mainly near the wave number of 3,560 cm^{-1}. According to FT-IR spectrum of KT, the content of silane coupling agent

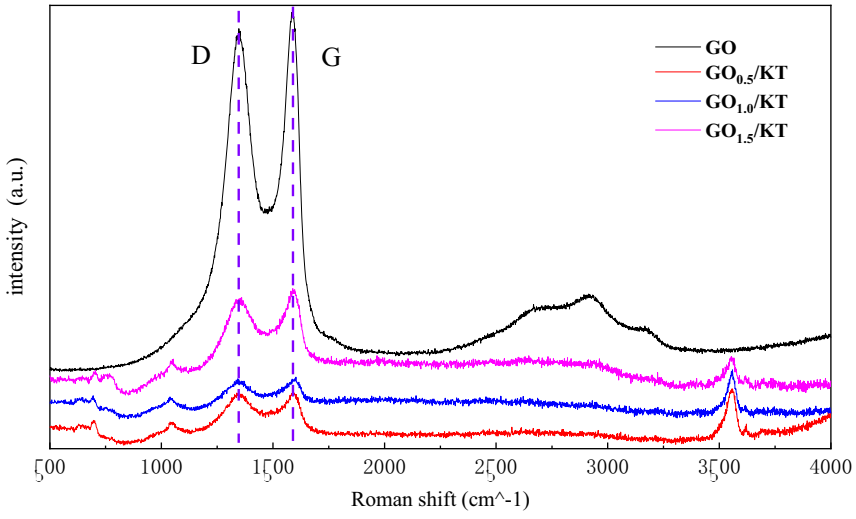

Figure 11: Raman spectra of GO/KT composites with different GO contents.

Table 8: Characteristic peaks of Raman spectra of GO and modified tourmaline

Materials	GO		$GO_{0.5}$/KT		$GO_{1.0}$/KT		$GO_{1.5}$/KT	
Characteristic peak	D	G	D	G	D	G	D	G
Frequency	1346.91	1587.29	1344.07	1591.42	1342.65	1602.42	1359.67	1588.67
Strength	21687.6	22599.9	2840.71	2867.82	2242.71	2335.07	5323.91	5827.03
I_D/I_G	0.960		0.991		0.960		0.914	

in modified tourmaline was very low after washing with alcohol and deionized water. It did not affect subsequent reactions. The main characteristic peaks of tourmaline did not change significantly before and after the reaction (surface modification and compounding). This indicated that GO does not have a significant effect on the structure of tourmaline during the electrostatic self-assembly process.

3.4 Adsorption properties of asphalt smoke

The smoke concentrations of base asphalt, KT-modified asphalt, and GO/KT-modified asphalt were tested, respectively. Their emission-reduction rates of asphalt smoke were calculated. The effect of the GO content on adsorption properties of tourmaline was assessed. The adsorption effects of different materials on asphalt smoke were shown in Figure 13.

From Figure 13, asphalt smoke concentration decreased sharply after the addition of tourmaline materials (KT and GO/KT). Moreover, with the increase of the GO content, asphalt smoke concentration decreased gradually. When the GO content was 1.5 wt%, the emission-reduction rate of asphalt smoke reached 41.11%. After adding GO, adsorption properties of tourmaline on asphalt smoke were improved. With the increase of the GO content, the improvement range gradually became flat. When the GO content was 1.5 wt%, the improvement was the largest, reaching 17.42%. Based on the above experimental results, it can be predicted that with the further increase of the GO content (>1.5 wt%), adsorption properties of tourmaline will continue to enhance. However, according to previous studies [46], if the content exceeds 1.5 wt%, the structure of G materials will be damaged to a certain extent during the preparation of composites. Therefore, the optimum content of GO was recommended to be 1.5 wt%.

Tourmaline has strong thermoelectric properties. When temperature changed, the crystal structure of tourmaline changed, resulting in the separation of positive and negative charges. It made tourmaline surface generate electric charge and has an adsorption effect on asphalt smoke [47]. GO had a strong ability of electron migration. When GO was compounded with tourmaline, it can

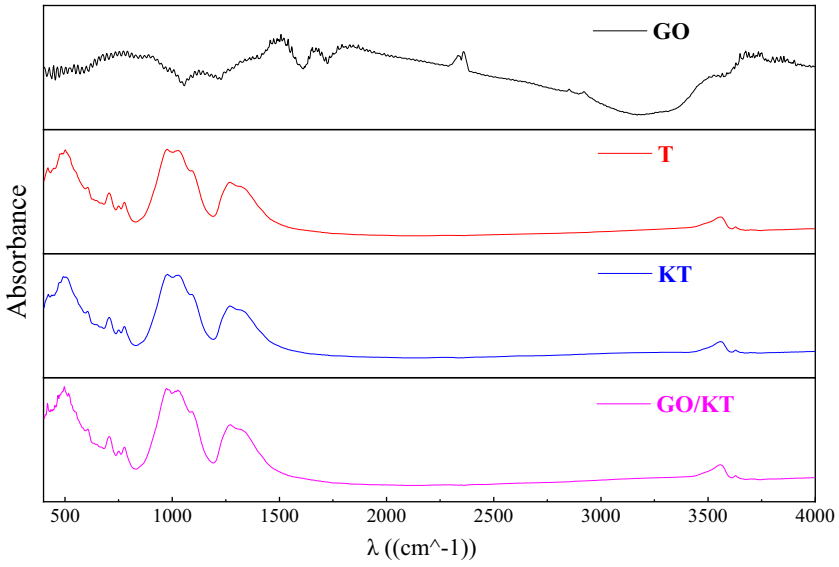

Figure 12: Infrared emission spectrum of different materials.

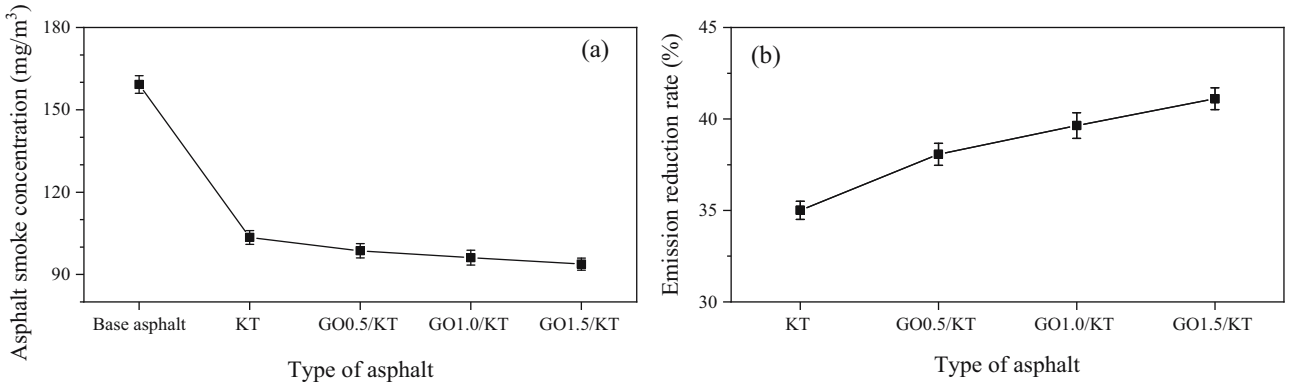

Figure 13: Asphalt smoke concentration (a) and emission reduction rate (b) of different types of asphalt.

promote the heteropolar charge around the tourmaline unit cell to leave the original position and promote the redistribution of positive and negative charges. The change of the whole dipole moment of tourmaline crystal was intensified. Then, the strength of surface electrostatic field increased [48]. In addition, the specific surface area of GO was much larger than that of tourmaline, which provides more adsorption sites. Therefore, the adsorption properties of tourmaline were improved.

4 Conclusion

(1) KH-550 was superior than CTAB in surface modification of tourmaline. After tourmaline was modified by KH-550, its zeta potential distribution shifted to the right and electrical property changed. The electrical property of KH-550-modified tourmaline was opposite to that of GO, which satisfied the requirements of electrostatic self-assembly method.

(2) According to material microanalysis methods of XRD, Raman spectroscopy and FT-IR, surface modification treatment did not change the structural characteristics of tourmaline. In addition, GO had no significant effect on the structure of tourmaline during the composite process.

(3) GO could enhance adsorption properties of tourmaline on asphalt smoke. When the GO content was 1.5 wt%, the improvement was the largest, which is 17.42%. At this time, the emission-reduction rate of asphalt smoke reached 41.11%.

(4) In this research, only the adsorption effect of composites on asphalt smoke has been studied, but the composition of asphalt smoke has not been analyzed. In the future, the adsorption effect and its durability of composites for nitrogen oxides and carbon oxides should be supplemented.

(5) GO, as a special material, will lead to high engineering cost when it is applied to pavement materials at this stage. Therefore, the influence of the type and content of nano-GO/tourmaline composites on the road performance of asphalt needs to be studied further. The optimum proportion of nano-GO/tourmaline composite should be considered according to road performance, environmental efficiency, and economy.

Funding information: This research was sponsored by the Key Research and Development Project in Shaanxi Province (2021GY-206) and Fundamental Research Funds for the Central Universities (300102219314). Their sponsorship and interest are gratefully acknowledged.

Author contributions: All authors have accepted responsibility for the entire content of this manuscript and approved its submission.

Conflict of interest: The authors state no conflict of interest.

References

[1] Wang C, Wang S, Gao Z, Song Z. Effect evaluation of road piezoelectric micro-energy collection-storage system based on laboratory and on-site tests. Appl Energ. 2021;287:116581.

[2] Khare P, Machesky J, Soto R, He M, Presto A, Gentner D. Asphalt-related emissions are a major missing source of secondary organic aerosol precursors. Sci Adv. 2020;6(36):eabb9785.

[3] Poulikakos L, Papadaskalopoulou C, Hofko B, Gschösser F, Falchetto A, Bueno M. Harvesting the unexplored potential of European waste materials for road construction. Resour Conserv Recy. 2017;116:32–44.
[4] Obrist M, Kannan R, Schmidt T, Kober T. Decarbonization pathways of the Swiss cement industry towards net zero emissions. J Clean Prod. 2021;288:125413.
[5] Zhang Z, Wang C, Zhang L, Wang S, Zen W. Construction and assessment technology of green road in China. J Chang'an Univ (Nat Sci Ed). 2018;38(5):76–86.
[6] Sun X, Yuan J, Zhang Y, Yin Y, Lv J, Jiang S. Thermal aging behavior characteristics of asphalt binder modified by nano-stabilizer based on DSR and AFM. Nanotechnol Rev. 2021;10(1):1157–82.
[7] Chen Q, Lu Y, Wang C, Han B, Fu H. Effect of raw material composition on the working performance of waterborne epoxy resin for road. Int J Pavement Eng. 2020;1–2. doi: 10.1080/10298436.2020.1856842.
[8] Zhang L. Preparation and properties of graphene/tourmaline composite modified asphalt materials. Master Dissertation. Xi'an City, Shaanxi Province, China: Chang'an University; 2019.
[9] Fu H, Wang C, Yu G, Chen Q, Liu L. Design optimization and performance evaluation of the open graded friction course with small particle size aggregate. Adv Civ Eng. 2021;2021:6668378.
[10] Wang C, Chen Q, Li QJ, Sun X, Li Z. A quantitative rating system for pollutant emission reduction of asphalt mixture. Math Probl Eng. 2017;2017:3761850.
[11] Ma C, Christianson L, Huang X, Christianson R, Li S. Efficacy of heated tourmaline in reducing biomass clogging within woodchip bioreactors. Sci Total Env. 2020;755:142401.
[12] Liang Y, Tang X, Zhu Q, Han J, Wang C. A review: application of tourmaline in environmental fields. Chemosphere. 2021;281(11):130780.
[13] Wang F, Meng J, Liang J, Fang B, Zhang H. Insight into the thermal behavior of tourmaline mineral. JOM. 2019;71:2468–74.
[14] Editorial Department of China Journal of Highway and Transport. Review on China's pavement engineering research-2020. China J Highway Transport. 2020;33(10):1–66.
[15] Ding H, Rahman A, Li Q, Qiu Y. Advanced mechanical characterization of asphalt mastics containing tourmaline modifier. Constr Build Mater. 2017;150:520–8.
[16] Ye Q, Dong W, Wang S, Li H. Research on the rheological characteristics and aging resistance of asphalt modified with tourmaline. Mater. 2020;13(1):69.
[17] Zhao Y, Wang P, Wang C, Li Y. Investigation of road performance and colloidal structure of tourmaline modified asphalt. Adv Mater Res. 2012;535–537:1731–4.
[18] Zhou X, Moghaddam T, Chen M, Wu S, Adhikari S. Biochar removes volatile organic compounds generated from asphalt. Sci Total Env. 2020;745:141096.
[19] Wang C, Wang P, Li Y, Zhao Y. Laboratory investigation of dynamic rheological properties of tourmaline modified bitumen. Constr Build Mater. 2015;80:195–9.
[20] Wang C, Fu H, Chen Q, Sun X, Guo T, Guo J. Preparation and performance of road micro-surfacing materials with exhaust purification function. KSCE J Civ Eng. 2019;23(7):2877–88.
[21] Chen Q, Wang C, Wen P, Wang M, Zhao J. Comprehensive performance evaluation of low-carbon modified asphalt based on efficacy coefficient method. J Clean Prod. 2018;203:633–44.
[22] Chen Q, Wang C, Wen P, Sun X, Guo T. Performance evaluation of tourmaline modified asphalt mixture based on grey target decision method. Constr Build Mater. 2019;205:137–47.
[23] Zhang X, Zhou X, Xu X, Zhang F, Chen L. Enhancing the functional and environmental properties of asphalt binders and asphalt mixtures using tourmaline anion powder modification. Coatings. 2021;11(5):550.
[24] Li G, Chen D, Zhao W, Zhang X. Efficient adsorption behavior of phosphate on la-modified tourmaline. J Environ Chem Eng. 2015;3(1):515–22.
[25] Li Y, Sun Y, Li J, Gao C. Socioeconomic drivers of urban heat island effect: empirical evidence from major Chinese cities. Sustain Cities Soc. 2020;63:102425.
[26] Chen Y, Wang S, Li Y, Liu Y, Zeng Z. Adsorption of Pb(II) by tourmaline-montmorillonite composite in aqueous phase. J Colloid Interf Sci. 2020;575:367–76.
[27] Li Y, Xing X, Pei J, Li R, Wen Y, Cui S, et al. Automobile exhaust gas purification material based on physical adsorption of tourmaline powder and visible light catalytic decomposition of g-C_3N_4/$BiVO_4$. Ceram Int. 2020;46(8):12637–47.
[28] Wang C, Chen Q, Guo T, Li Q. Environmental effects and enhancement mechanism of graphene/tourmaline composites. J Clean Prod. 2020;262:121313.
[29] Sun L, Guo Y, Hu Y, Pan S, Jiao Z. Conductometric n-butanol gas sensor based on Tourmaline@ZnO hierarchical micro-nanostructures. Sens Actuat B-Chem. 2021;337:129793.
[30] Zhang X, Jing Q, Ao S, Schneider GF, Kireev D, Zhang Z, et al. Ultrasensitive field-effect biosensors enabled by the unique electronic properties of graphene. Small. 2020;16(15):1902820.
[31] Sherlala A, Raman A, Bello MM, Asghar A. A review of the applications of organo-functionalized magnetic graphene oxide nanocomposites for heavy metal adsorption. Chemosphere. 2018;193:1004–17.
[32] Zhang X, Wang Y, Luo G, Xing M. Two-dimensional graphene family material: assembly, biocompatibility and sensors applications. Sensors-Basel. 2019;19(13):2966.
[33] Phasuksom K, Prissanaroon-Ouajai W, Sirivat A. A highly responsive methanol sensor based on graphene oxide/polyindole composites. RSC Adv. 2020;10(26):15206–20.
[34] Korkmaz S, Kariper A. Graphene and graphene oxide based aerogels: Synthesis, characteristics and supercapacitor applications. J Energy Storage. 2020;27:101038.
[35] Deng P, Liu Y, Luo P, Wang J, Liu Y, Wang D, et al. Two-steps synthesis of sandwich-like graphene oxide/LLM-105 nanoenergetic composites using functionalized graphene. Mater Lett. 2017;194:156–9.
[36] Wang J, Lei W, Xue Z, Qian H, Liu W. Research progress on synthesis and application of graphene reinforced metal matrix composites. J Mater Eng. 2018;46(12):18–27.
[37] Guo T, Wang C, Chen H, Li Z, Chen Q, Han A, et al. Rheological properties of graphene-tourmaline composite modified asphalt. Pet Sci Technol. 2019;37(21):2190–8.
[38] Zhang D, Shen H, Cao X, Ye Y, Zhang X, Ye L, et al. Research progress in graphene reinforced aeronautical metal matrix composites. J Mater Eng. 2019;47(1):1–10.
[39] Chen Q, Wang C, Qiao Z, Guo T. Graphene/tourmaline composites as a filler of hot mix asphalt mixture: preparation and properties. Constr Build Mater. 2020;239:117859.

[40] Luo Y, Chen Q, Wang C, Guo T. Preparation and improved negative ion release of graphene/tourmaline composite. Mater Res Express. 2019;6:055507.
[41] Ministry of Ecology and Environment of the People's Republic of China. Emission standard of pollutants for petroleum refining industry. GB 31570–2015. Beijing: China Environmental Science Press; 2015.
[42] Lin S, Sun S, Shen K, Dong F. Environmental functionalities of tourmaline and applications of its functional composites. Mater Rev. 2017;31(7):131–7.
[43] Zhang S, Sun J, Hu D, Xiao C, Zhuo Q, Wang J, et al. Large-sized graphene oxide/modified tourmaline nanoparticle aerogel with stable honeycomb-like structure for high-efficiency PM2.5 capture. J Mater Chem A. 2018;6:16139–48.
[44] Huang Z, Wang T, Zhang X, Zheng L, Xue G, Liang J. Preparation of tourmaline/graphene oxide and its application in thermal interface materials. J Compos Mater. 2016;50(28):3953–60.
[45] Zhang K, Wang J, Fei G, Xia H. Properties of natural rubber filled with graphene oxide and mesoporous silica. Polym Mater Sci Eng. 2018;34(8):117–23.
[46] Guo T, Fu H, Wang C, Chen H, Chen Q, Wang Q, et al. Road performance and emission reduction effect of graphene/tourmaline-composite-modified asphalt. Sustainability. 2021;13(16):8932.
[47] Yin D, Yu M, Shi J, Xu Z, Song D, Liu G. Adsorption characteristics of enrofloxacin by schorl. Chin J Environ Eng. 2017;11(4):2183–9.
[48] Bronzova Y, Babushkina M, Frank-Kamenetskaya O, Vereshchagin O, Rozhdestvenskaya I, Zolotarev A. Short-range order in Li–Al tourmalines: IR spectroscopy, X-ray single crystal diffraction analysis and a bond valence theory approach. Phys Chem Min. 2019;46(9):815–25.